

Hypergraph Motifs: Concepts, Algorithms, and Discoveries

Geon Lee
KAIST, South Korea
geonlee0325@kaist.ac.kr

Jihoon Ko
KAIST, South Korea
jihoonko@kaist.ac.kr

Kijung Shin
KAIST, South Korea
kijung@kaist.ac.kr

ABSTRACT

Hypergraphs naturally represent group interactions, which are omnipresent in many domains: collaborations of researchers, co-purchases of items, joint interactions of proteins, to name a few. In this work, we propose tools for answering the following questions in a systematic manner: **(Q1)** what are structural design principles of real-world hypergraphs? **(Q2)** how can we compare local structures of hypergraphs of different sizes? **(Q3)** how can we identify domains which hypergraphs are from? We first define *hypergraph motifs* (h-motifs), which describe the connectivity patterns of three connected hyperedges. Then, we define the significance of each h-motif in a hypergraph as its occurrences relative to those in properly randomized hypergraphs. Lastly, we define the *characteristic profile* (CP) as the vector of the normalized significance of every h-motif. Regarding Q1, we find that h-motifs' occurrences in 11 real-world hypergraphs from 5 domains are clearly distinguished from those of randomized hypergraphs. In addition, we demonstrate that CPs capture local structural patterns unique in each domain, and thus comparing CPs of hypergraphs addresses Q2 and Q3. Our algorithmic contribution is to propose MoCHy, a family of parallel algorithms for counting h-motifs' occurrences in a hypergraph. We theoretically analyze their speed and accuracy, and we show empirically that the advanced approximate version MoCHy-A⁺ is up to 25× more accurate and 32× faster than the basic approximate and exact versions, respectively.

1. INTRODUCTION

Complex systems consisting of pairwise interactions between individuals or objects are naturally expressed in the form of graphs. Nodes and edges, which compose a graph, represent individuals (or objects) and their pairwise interactions, respectively. Thanks to their powerful expressiveness, graphs have been used in a wide variety of fields, including social network analysis, web, bioinformatics, and epidemiology. Global structural patterns of real-world graphs, such as power-law degree distribution and [8, 18], and six degrees of separation [28, 60], have been extensively investigated.

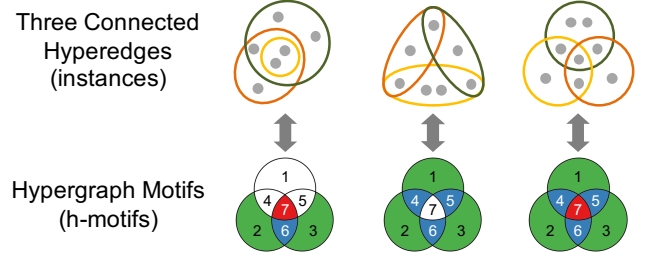


Figure 1: Example hyperedge motifs (or h-motifs in short) (below) and their instances (above).

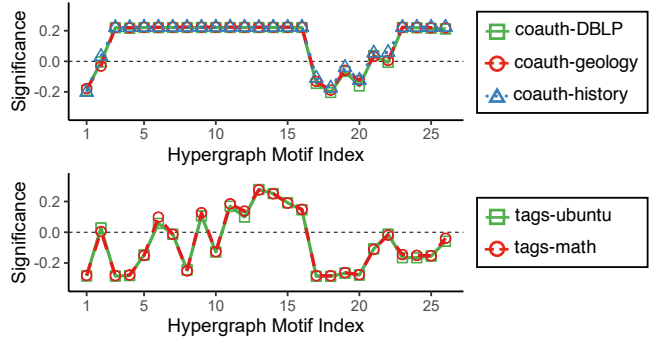


Figure 2: Distributions of h-motifs' instances precisely characterize local structural patterns of real-world hypergraphs. Note that the hypergraphs from the same domains have similar distributions, while the hypergraphs from different domains do not. See Section 5.3 for details.

In addition to global patterns, real-world graphs exhibit patterns in their local structures, which differentiate graphs in the same domain from random graphs or those in other domains. Local structures are revealed by counting the occurrences of different network motifs [41, 42], which describe the connectivity pattern of pairwise interactions between a fixed number of connected nodes (typically 3, 4, or 5 nodes). As a fundamental building block, network motifs have played a key role in many analytical and predictive tasks, including community detection [11, 39, 57, 62], classification [16, 34, 41], and anomaly detection [9, 52].

Despite the prevalence of graphs, interactions in many complex systems are groupwise rather than pairwise: collaborations of researchers, co-purchases of items, joint interactions of proteins, tags attached to the same web post, to name a few. These group interactions cannot be represented by edges in a graph. Suppose three or more researchers coauthor a publication. This co-authorship cannot be rep-

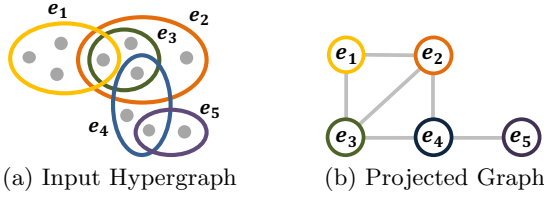


Figure 3: A hypergraph and its projected graph. Hyperedges in the hypergraph act as nodes in the projected graph.

represented as a single edge, and creating edges between all pairs of the researchers cannot be distinguished from multiple papers coauthored by subsets of the researchers.

This inherent limitation of graphs is addressed by hypergraphs, which consist of nodes and hyperedges. Each hyperedge is a subset of any number of nodes, and it represents a group interaction among the nodes. For example, in a hypergraph, a paper coauthored by three researchers a , b , and c is expressed as a hyperedge $\{a, b, c\}$, and it is distinguished from three papers coauthored by each pair, which are represented as three hyperedges $\{a, b\}$, $\{b, c\}$, and $\{c, a\}$.

The successful investigation and discovery of local structural patterns in real-world graphs motivates us to explore local structural patterns in real-world hypergraphs. However, network motifs, which proved to be useful for graphs, are not trivially extended to hypergraphs. Specifically, due to the flexibility in the size of hyperedges, there can be infinitely many connectivity patterns of interactions among a fixed number of nodes, and other nodes can also be associated with these interactions.

In this work, taking these challenges into consideration, we define 26 *hypergraph motifs* (h-motifs) so that they describe connectivity patterns of three connected hyperedges (rather than nodes). As seen in Figure 1, h-motifs describe the connectivity pattern of hyperedges A , B , and C by the emptiness of the 7 subsets: $A \setminus B \setminus C$, $B \setminus C \setminus A$, $C \setminus A \setminus B$, $A \cap B \setminus C$, $B \cap C \setminus A$, $C \cap A \setminus B$, and $A \cap B \cap C$. As a result, every connectivity pattern is described by a unique h-motif, independently of the sizes of hyperedges. While this work focuses on connectivity patterns of three hyperedges, h-motifs are easily extended to four or more hyperedges.

We count the number of each h-motif’s instances in 11 real-world hypergraphs from 5 different domains. Then, we measure the significance of each h-motif in each hypergraph by comparing the count of its instances in the hypergraph against the counts in properly randomized hypergraphs. Lastly, we compute the *characteristic profile* (CP) of each hypergraph, defined as the vector of the normalized significance of every h-motif. Comparing the counts and CPs of different hypergraphs leads to the following observations:

- Structural design principles of real-world hypergraphs that are captured by frequencies of different h-motifs are clearly distinguished from those of randomized hypergraphs.
- Hypergraphs from the same domains have similar CPs, while hypergraphs from different domains have distinct CPs (see Figure 2). In other words, CPs successfully captures local structure patterns unique in each domain.

Our algorithmic contribution is to design **MoCHy** (**Motif Counting in Hypergraphs**), a family of parallel algorithms for counting h-motifs’ instances, which is the computational bottleneck of the above process. Note that since non-pairwise

interactions (e.g., intersection of three hyperedges) are taken into consideration, counting the instances of h-motifs is more challenging than counting the instances of network motifs, which are defined solely based on pairwise interactions. We provide one exact version, named **MoCHy-E**, and two approximate versions, named **MoCHy-A** and **MoCHy-A⁺**. Empirically, **MoCHy-A⁺** is up to $25\times$ more accurate than **MoCHy-A**, and it is up to $32\times$ faster than **MoCHy-E**, with little sacrifice of accuracy. These empirical results are consistent with our theoretical analysis of their speed, bias, and variance.

In summary, our contributions are summarized as follow:

- **Novel Concepts:** We propose h-motifs, the counts of whose instances capture local structures of hypergraphs, independently of the sizes of hyperedges or hypergraphs.
- **Fast and Provable Algorithms:** We develop **MoCHy**, a family of parallel algorithms for counting h-motifs’ instances. We show theoretically and empirically that the advanced version significantly outperforms the basic ones, providing a better trade-off between speed and accuracy.
- **Discoveries in 11 Real-world Hypergraphs:** We show that h-motifs and CPs reveal local structural patterns that are shared by hypergraphs from the same domains but distinguished from those of random hypergraphs and hypergraphs from other domains (see Figure 2).

In Section 2, we discuss related works. In Section 3, we introduce h-motifs and characteristic profiles. In Section 4, we present exact and approximate algorithms for counting instances of h-motifs, and we analyze their theoretical properties. After providing experimental results in Section 5, we offer conclusions in Section 6.

2. RELATED WORK

In this section, we review previous work on network motifs, algorithms for network motif counting, and hypergraphs. While the definition of a network motif varies among studies, here we define it as a connected graph composed by a predefined number of nodes.

Network Motifs. Network motifs were proposed as a tool for understanding the underlying design principles and capturing the local structural patterns of graphs [19, 50, 42]. The occurrences of motifs in real-world graphs are significantly different from those in random graphs [42] and also vary depending on the domains of graphs [41]. The concept of network motifs has been extended to various types of graphs, including dynamic [45], bipartite [13], and heterogeneous [47] graphs. The occurrences of network motifs have been used in a wide range of graph applications: community detection [11, 62, 39, 57], ranking [67], graph embedding [48, 65], and graph neural networks [34], to name a few.

Algorithms for Network Motif Counting. Due to these wide applications, numerous algorithms have been proposed for rapid and accurate counting of the occurrences of motifs in large graphs. Some of them focus on counting the occurrences of a particular motif, such as the triangle (i.e., clique of three nodes) [2, 17, 20, 21, 26, 31, 33, 44, 51, 52, 56, 58, 59], the butterfly (i.e., 2×2 biclique) [49], and the clique of k nodes [25]. Others are for counting the occurrences of every motif of a fixed size [3, 4, 7, 14, 46]. Many of these algorithms employ sampling to estimate the counts [2, 7, 14, 17,

Table 1: Frequently-used symbols.

Notation	Definition
$G = (V, E)$	hypergraph with nodes V and hyperedges E
$E = \{e_1, \dots, e_{ E }\}$	set of hyperedges
E_v	set of hyperedges that contains a node v
\wedge	set of hyperwedges in G
\wedge_{ij}	hyperwedge consisting of e_i and e_j
$\tilde{G} = (E, \wedge, \omega)$	projected graph of G
$\omega(\wedge_{ij})$	the number of nodes shared between e_i and e_j
N_{e_i}	set of neighbors of e_i in \tilde{G}
$h(\{e_i, e_j, e_k\})$	h-motif corresponding to an instance $\{e_i, e_j, e_k\}$
$M[t]$	count of h-motif t 's instances

26, 44, 49, 51, 52, 56]. Note that these previous approaches for counting the occurrences of network motifs are not directly applicable to the problem of counting the occurrences of h-motifs. This is because different from network motifs, which are defined solely based on pairwise interactions, h-motifs are defined based on non-pairwise interactions (see Section 3.2).

Hypergraph. Hypergraphs naturally represent group interactions, and they have been identified as a useful tool in a wide range of fields, including computer vision [23, 22, 64], bioinformatics [24], circuit design [29, 43], social network analysis [61, 36], and recommender systems [15, 37]. There also has been considerable attention on machine learning on hypergraphs, including clustering [1, 6, 30, 38, 68], classification [27, 55, 64] and hyperedge prediction [10, 63, 66]. Recently, empirical studies on real-world hypergraphs have revealed several structural and temporal patterns [10, 12]. They focus on simplicial closure (i.e., the emergence of the first hyperedge that includes a set of nodes each of whose pairs co-appear in previous hyperedges) [10] and repetition of the same hyperedges and their subsets [12].

3. PROPOSED CONCEPTS

In this section, we introduce the proposed concepts: hypergraph motifs and characteristic profiles. Refer Table 1 for the notations frequently used throughout the paper.

3.1 Preliminaries and Notations

We define some preliminary concepts and their notations.

Hypergraph Consider a *hypergraph* $G = (V, E)$, where V and $E := \{e_1, e_2, \dots, e_{|E|}\}$ are sets of nodes and hyperedges, respectively. Each hyperedge $e_i \in E$ is a non-empty subset of V , and we use $|e_i|$ to denote the number of nodes in it. For each node $v \in V$, we use $E_v := \{e_i \in E : v \in e_i\}$ to denote the set of hyperedges that include v . We say two hyperedges e_i and e_j are *adjacent* if they share any member, i.e., if $e_i \cap e_j \neq \emptyset$. Then, for each hyperedge e_i , we denote the set of hyperedges adjacent to e_i as $N_{e_i} := \{e_j \in E : e_i \cap e_j \neq \emptyset\}$ and the number of such hyperedges as $|N_{e_i}|$. Similarly, we say three hyperedges e_i , e_j , and e_k are *connected* if one of them is adjacent to two the others.

Hyperwedges: We define a *hyperwedge* as an unordered pair of adjacent hyperedges. We denote the set of hyperwedges in G by $\wedge := \{\{e_i, e_j\} \in \binom{E}{2} : e_i \cap e_j \neq \emptyset\}$. We use $\wedge_{ij} \in \wedge$ to denote the hyperwedge consisting of e_i and e_j . In the example hypergraph in Figure 3(a), there are six hyperwedges: \wedge_{12} , \wedge_{13} , \wedge_{23} , \wedge_{24} , \wedge_{34} , and \wedge_{45} .

Projected Graph: We define the *projected graph* of $G = (V, E)$ by $\tilde{G} = (E, \wedge, \omega)$, where \wedge is the set of hyperwedges and $\omega(\wedge_{ij}) := |e_i \cap e_j|$. That is, in the projected graph \tilde{G} , hyperedges in G act as nodes, and two of them are adjacent if and only if they share any member. Note that for each hyperedge $e_i \in E$, N_{e_i} is the set of neighbors of e_i in \tilde{G} , and $|N_{e_i}|$ is its degree in \tilde{G} . Figure 3(b) shows the projected graph of the example hypergraph in Figure 3(a).

3.2 Hypergraph Motifs

We introduce hypergraph motifs, which are basic building blocks of hypergraphs, with related concepts. Then, we discuss their properties and generalization.

Definition and Representation: Hypergraph motifs (or h-motifs in short) are for describing the connectivity patterns of three connected hyperedges. Specifically, given a set $\{e_i, e_j, e_k\}$ of three connected hyperedges, h-motifs describe its connectivity pattern by the emptiness of the following seven sets: (1) $e_i \setminus e_j \setminus e_k$, (2) $e_j \setminus e_k \setminus e_i$, (3) $e_k \setminus e_i \setminus e_j$, (4) $e_i \cap e_j \setminus e_k$, (5) $e_j \cap e_k \setminus e_i$, (6) $e_k \cap e_i \setminus e_j$, and (7) $e_i \cap e_j \cap e_k$. Formally, a h-motif is defined as a binary vector of size 7 whose elements represent the emptiness of the above sets, resp., and as seen in Figure 1, h-motifs are naturally represented in the Venn diagram. While there can be 2^7 h-motifs, 26 h-motifs remain once we exclude symmetric ones, those with duplicated hyperedges (see Figure 5), and those cannot be obtained from connected hyperedges. The 26 cases, which we call *h-motif 1* through *h-motif 26*, are visualized in the Venn diagram in Figure 4.

Instances, Open h-motifs, and Closed h-motifs: Consider a hypergraph $G = (V, E)$. A set of three connected hyperedges is an *instance* of h-motif t if their connectivity pattern corresponds to h-motif t . The count of each h-motif's instances is used to characterize the local structure of G , as discussed in the following sections. A h-motif is *closed* if all three hyperedges in its instances are adjacent to (i.e., overlapped with) each other. If its instances contain two non-adjacent (i.e., disjoint) hyperedges, a h-motif is *open*. In Figure 4, h-motifs 17 - 22 are open; the others are closed.

Properties of h-motifs: From the definition of h-motifs, the following desirable properties, which are discussed in Section 1, are immediate:

- **Exhaustive:** h-motifs capture connectivity patterns of *all possible* three connected hyperedges.
- **Unique:** connectivity pattern of any three connected hyperedges is captured by *exactly one* h-motif.
- **Size Independent:** h-motifs capture connectivity patterns *independently of the sizes of hyperedges*. Note that there can be infinitely many combinations of sizes of three connected hyperedges.

Generalization to Four or More Hyperedges: The concept of h-motifs is easily generalized to four or more hyperedges. For example, a h-motif for four hyperedges can be defined as a binary vector of size 15 indicating the emptiness of each region in the Venn diagram for four sets. We leave this generalization as future work and focus on the h-motifs for three hyperedges since they are already capable of characterizing local structures of real-world hypergraphs, as shown empirically in Section 5.

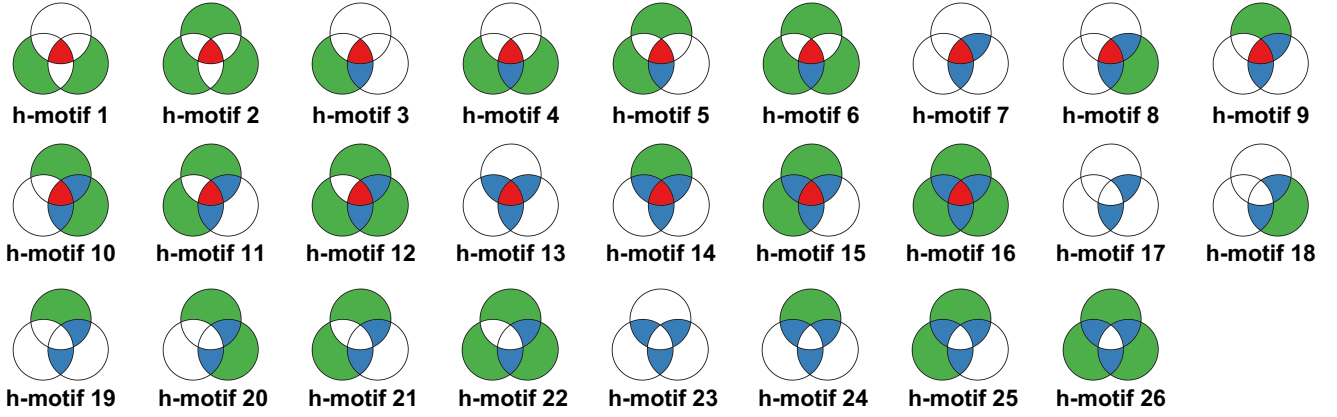


Figure 4: The 26 h-motifs studied in this work. Note that h-motifs 17 - 22 are open, while the others are closed.

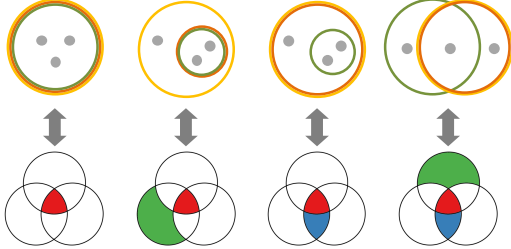


Figure 5: The h-motifs (below) whose instances (above) contain duplicated hyperedges.

3.3 Characteristic Profile (CP)

What are the structural design principles of real-world hypergraphs distinguished from those of random hypergraphs? Below, we introduce the characteristic profile (CP), which is a tool for answering the above question using h-motifs.

Randomized Hypergraphs: While one might try to characterize the local structure of a hypergraph by absolute counts of each h-motifs' instances in it, some h-motifs may naturally have many instances. Thus, for more accurate characterization, we need random hypergraphs to be compared against real-world hypergraphs. We obtain such random hypergraphs by randomizing a compared real-world hypergraph. To this end, we represent the hypergraph $G = (V, E)$ as a bipartite graph where V and E are the two partitions of nodes, and there exists an edge between $v \in V$ $e \in E$ if and only if $v \in e$. Then, we use the Chung-Lu bipartite graph generative model, which successfully preserves the degree distribution [5]. As a result, we obtain randomized hypergraphs in which the degree (i.e., the number of hyperedges that each node belongs to) distribution of nodes and the size distribution of hyperedges in G are maintained.

Significance of H-motifs: We measure the significance of each h-motif in a hypergraph by comparing the count of its instances against the count of them in random hypergraphs. Specifically, the *significance* of a h-motif t in a hypergraph G is defined as

$$\Delta_t := \frac{M[t] - M_{rand}[t]}{M[t] + M_{rand}[t] + \epsilon}, \quad (1)$$

where $M[t]$ is the number of instances of h-motif t in G , and $M_{rand}[t]$ is the average number of instances of h-motif t randomized hypergraphs obtained as described above. We fixed ϵ to 1 throughout this paper. This way of measuring significance was proposed in [42] for network motifs as an alternative of normalized Z scores, which heavily depend on

the graph size.

Characteristic Profile (CP): By normalizing and concatenating the significances of all h-motifs in a hypergraph, we obtain the characteristic profile (CP), which summarizes the local structural pattern in the hypergraph. Specifically, the *characteristic profile* of a hypergraph in G is a vector of size 26, where each t -th element is

$$CP_t := \frac{\Delta_t}{\sqrt{\sum_{t=1}^{26} \Delta_t^2}}. \quad (2)$$

Note that, for each t , CP_t is between -1 and 1 . The CP is used in Section 5.3 to compare the local structural patterns of real-world hypergraphs from diverse domains.

4. PROPOSED ALGORITHMS

Given a hypergraph, how can we count the instances of each h-motif? Once we count them in the original and randomized hypergraphs, the significance of each motif and the CP are obtained immediately by Eq. (1) and Eq. (2).

The problem of counting of h-motifs' instances bears some similarity to the classic problem of counting network motifs' instances. However, different from network motifs, which are defined solely based on pairwise interactions, h-motifs are defined based on non-pairwise interactions (e.g., $e_i \cap e_j \cap e_k$). Due to this difference, new approaches are required.

In this section, we present MoCHy (Motif Counting in Hypergraphs), which is a family of parallel algorithms for counting the instances of each h-motif in the input hypergraph. We first describe hypergraph projection, which is a preprocessing step of every version of MoCHy. Then, we present MoCHy-E, which is for exact counting. After that, we present two different versions of MoCHy-A, which are sampling-based algorithms for approximate counting. Lastly, we discuss parallel and on-the-fly implementations.

Throughout this section, we use $h(\{e_i, e_j, e_k\})$ to denote the h-motif that describes the connectivity pattern of an h-motif instance $\{e_i, e_j, e_k\}$. We also use $M[t]$ to denote the count of instances of h-motif t .

4.1 Hypergraph Projection (Algorithm 1)

As a preprocessing step, every version of MoCHy builds the projected graph $\bar{G} = (E, \wedge, \omega)$ (see Section 3.1) of the input hypergraph $G = (V, E)$, as described in Algorithm 1. To find the neighbors of each hyperedge e_i (line 3), the algorithm visits each hyperedge e_j that contains v and satisfies $j > i$ (line 5) for each node $v \in e_i$ (line 4). Then for each

Algorithm 1: Hypergraph Projection (Preprocess)

Input : input hypergraph: $G = (V, E)$
Output: projected graph: $\tilde{G} = (E, \wedge, \omega)$

```
1  $\wedge \leftarrow \emptyset$ 
2  $\omega \leftarrow$  map whose default value is 0
3 for each hyperedge  $e_i \in E$  do
4   for each node  $v \in e_i$  do
5     for each hyperedge  $e_j \in E_v$  where  $j > i$  do
6        $\wedge \leftarrow \wedge \cup \{\wedge_{ij}\}$ 
7        $\omega(\wedge_{ij}) = \omega(\wedge_{ij}) + 1$ 
8     end
9   end
10 end
11 return  $\tilde{G} = (E, \wedge, \omega)$ 
```

such e_j , it adds $\wedge_{ij} = \{e_i, e_j\}$ to \wedge and increments $\omega(\wedge_{ij})$ (lines 6 and 7). The time complexity of this preprocessing step is given in Lemma 1.

Lemma 1 (Complexity of Hypergraph Projection). *The time complexity of Algorithm 1 is $O(\sum_{\wedge_{ij} \in \wedge} |e_i \cap e_j|)$.*

Proof. If all sets and maps are implemented using hash tables, lines 6 and 7 take $O(1)$ time, and they are executed $|e_i \cap e_j|$ times for each $\wedge_{ij} \in \wedge$. \square

Since $|\wedge| < \sum_{e_i \in E} |N_{e_i}|$ and $|e_i \cap e_j| \leq |e_i|$, Eq. (3) holds.

$$\sum_{\wedge_{ij} \in \wedge} |e_i \cap e_j| < \sum_{e_i \in E} (|e_i| \cdot |N_{e_i}|). \quad (3)$$

4.2 Exact H-motif Counting (Algorithm 2)

We present MoCHy-E (MoCHy **E**xact), which exactly count the instances of each h-motif. The procedures of MoCHy-E are described in Algorithm 2. For each hyperedge $e_i \in E$ (line 2), each unordered pair $\{e_j, e_k\}$ of its neighbors, which forms an h-motif instance $\{e_i, e_j, e_k\}$, is considered (line 3). If $e_j \cap e_k = \emptyset$ (i.e., if the corresponding h-motif is open), $\{e_i, e_j, e_k\}$ is considered only once. However, if $e_j \cap e_k \neq \emptyset$ (i.e., if the corresponding h-motif is closed), $\{e_i, e_j, e_k\}$ is considered two more times (i.e., when e_j is chosen in line 2 and when e_k is chosen in line 2). Based on these observations, given an h-motif instance $\{e_i, e_j, e_k\}$, the corresponding count $M[h(\{e_i, e_j, e_k\})]$ is incremented (line 5) only if $e_j \cap e_k = \emptyset$ or $i < \min(j, k)$ (line 4). This guarantees that each $\{e_i, e_j, e_k\}$ is counted exactly once. The time complexity of MoCHy-E is given in Theorem 1, which is based on Lemma 2.

Lemma 2 (Time Complexity of Computing $h(\{e_i, e_j, e_k\})$). *Given the input hypergraph $G = (V, E)$ and its projected graph $\tilde{G} = (E, \wedge, \omega)$, for each h-motif instance $\{e_i, e_j, e_k\}$, computing $h(\{e_i, e_j, e_k\})$ takes $O(\min(|e_i|, |e_j|, |e_k|))$ time.*

Proof. Assume $|e_i| = \min(|e_i|, |e_j|, |e_k|)$, without loss of generality, and all sets and maps are implemented using hash tables. As defined in Section 3.2, $h(\{e_i, e_j, e_k\})$ is computed in $O(1)$ time from the emptiness of the following sets: (1) $e_i \setminus e_j \setminus e_k$, (2) $e_j \setminus e_k \setminus e_i$, (3) $e_k \setminus e_i \setminus e_j$, (4) $e_i \cap e_j \setminus e_k$, (5) $e_j \cap e_k \setminus e_i$, (6) $e_k \cap e_i \setminus e_j$, and (7) $e_i \cap e_j \cap e_k$. We check their emptiness from their cardinalities. We obtain e_i , e_j , and e_k , which are stored in G , and their cardinalities in $O(1)$ time.

Algorithm 2: MoCHy-E: Exact H-motif Counting

Input : (1) input hypergraph: $G = (V, E)$
(2) projected graph: $\tilde{G} = (E, \wedge, \omega)$
Output: exact count of each h-motif t 's instances: $M[t]$

```
1  $M \leftarrow$  map whose default value is 0
2 for each hyperedge  $e_i \in E$  do
3   for each unordered hyperedge pair  $\{e_j, e_k\} \in \binom{N_{e_i}}{2}$  do
4     if  $e_j \cap e_k = \emptyset$  or  $i < \min(j, k)$  then
5        $M[h(\{e_i, e_j, e_k\})] += 1$ 
6     end
7   end
8 end
9 return  $M$ 
```

Similarly, we obtain $|e_i \cap e_j|$, $|e_j \cap e_k|$, and $|e_k \cap e_i|$, which are stored in \tilde{G} , in $O(1)$ time. Then, we compute $|e_i \cap e_j \cap e_k|$ in $O(|e_i|)$ time by checking for each node in e_i whether it is also in both e_j and e_k . From these cardinalities, we obtain the cardinalities of the six other sets in $O(1)$ time as follows:

- (1) $|e_i \setminus e_j \setminus e_k| = |e_i| - |e_i \cap e_j| - |e_k \cap e_i| + |e_i \cap e_j \cap e_k|$,
- (2) $|e_j \setminus e_k \setminus e_i| = |e_j| - |e_i \cap e_j| - |e_j \cap e_k| + |e_i \cap e_j \cap e_k|$,
- (3) $|e_k \setminus e_i \setminus e_j| = |e_k| - |e_k \cap e_i| - |e_j \cap e_k| + |e_i \cap e_j \cap e_k|$,
- (4) $|e_i \cap e_j \setminus e_k| = |e_i \cap e_j| - |e_i \cap e_j \cap e_k|$,
- (5) $|e_j \cap e_k \setminus e_i| = |e_j \cap e_k| - |e_i \cap e_j \cap e_k|$,
- (6) $|e_k \cap e_i \setminus e_j| = |e_k \cap e_i| - |e_i \cap e_j \cap e_k|$.

Hence, the time complexity of computing $h(\{e_i, e_j, e_k\})$ is $O(|e_i|) = O(\min(|e_i|, |e_j|, |e_k|))$. \square

Theorem 1 (Complexity of MoCHy-E). *The time complexity of Algorithm 2 is $O(\sum_{e_i \in E} (|N_{e_i}|^2 \cdot |e_i|))$.*

Proof. Assume all sets and maps are implemented using hash tables. The total number of triples $\{e_i, e_j, e_k\}$ considered in line 3 is $O(\sum_{e_i \in E} |N_{e_i}|^2)$. By Lemma 2, for such a triple $\{e_i, e_j, e_k\}$, computing $h(\{e_i, e_j, e_k\})$ takes $O(|e_i|)$ time. Thus, the total time complexity of Algorithm 2 is $O(\sum_{e_i \in E} (|e_i| \cdot |N_{e_i}|^2))$, which upper bounds that of the preprocessing step (see Lemma 1 and Eq. (3)). \square

4.3 Approximate H-motif Counting

We present two different versions of MoCHy-A (MoCHy **A**pproximate), which approximately count the instances of each h-motif. Both versions estimate the counts by exploring the input hypergraph partially through hyperedge and hyperwedge sampling, resp., and thus they are particularly useful for large-scale hypergraphs. In addition, both versions yield unbiased estimates.

MoCHy-A: Hyperedge Sampling (Algorithm 3):

MoCHy-A, which is based on hyperedge sampling, is described in Algorithm 3. It repeatedly samples s hyperedges from the hyperedge set E uniformly at random with replacement (line 3). For each sampled hyperedge e_i , the algorithm searches for all h-motif instances that contain e_i (lines 4-9), and to this end, the 1-hop and 2-hop neighbors of e_i in the projected graph \tilde{G} are explored. After that, for each such instance $\{e_i, e_j, e_k\}$ of h-motif t , the corresponding count $\bar{M}[t]$ is incremented (line 6). Lastly, each estimate $\bar{M}[t]$ is

Algorithm 3: MoCHy-A: Approximate H-motif Counting Based on Hyperedge Sampling

Input : (1) input hypergraph: $G = (V, E)$
(2) projected graph: $\bar{G} = (E, \wedge, \omega)$
(3) number of samples: s

Output: estimated count of each h-motif t 's instances: $\bar{M}[t]$

```

1  $\bar{M}[t] \leftarrow$  map whose default value is 0
2 for  $n \leftarrow 1 \dots s$  do
3    $e_i \leftarrow$  sample a uniformly random hyperedge
4   for each hyperedge  $e_j \in N_{e_i}$  do
5     for each hyperedge  $e_k \in (N_{e_i} \cup N_{e_j} \setminus \{e_i, e_j\})$  do
6        $\bar{M}[h(\{e_i, e_j, e_k\})] += 1$ 
7     end
8   end
9 end
10 for each h-motif  $t$  do
11    $\bar{M}[t] \leftarrow \bar{M}[t] \cdot \frac{|E|}{3s}$ 
12 end
13 return  $\bar{M}$ 

```

rescaled by multiplying it with $\frac{|E|}{3s}$ (lines 10-12), which is the reciprocal of the expected number of times that each of the h-motif t 's instances is counted. Note that each hyperedge is expected to be sampled $\frac{s}{|E|}$ times, and each h-motif instance is counted whenever any of its three hyperedges is sampled. This rescaling makes each estimate $\bar{M}[t]$ unbiased, as formalized in Theorem 2.

Theorem 2 (Bias and Variance of MoCHy-A). *For every h-motif t , Algorithm 3 provides an unbiased estimate $\bar{M}[t]$ of the count $M[t]$ of its instances, i.e.,*

$$\mathbb{E}[\bar{M}[t]] = M[t]. \quad (4)$$

The variance of the estimate is

$$\text{Var}[\bar{M}[t]] = \frac{1}{3s} \cdot M[t] \cdot (|E| - 3) + \frac{1}{9s} \sum_{l=0}^2 p_l[t] \cdot (l|E| - 9), \quad (5)$$

where $p_l[t]$ is the number of pairs of h-motif t 's instances that share l hyperedges.

Proof. See Appendix A. \square

The time complexity of MoCHy-A is given in Theorem 3.

Theorem 3 (Complexity of MoCHy-A). *The average time complexity of Algorithm 3 is $O(\frac{s}{|E|} \sum_{e_i \in E} (|e_i| \cdot |N_{e_i}|^2))$.*

Proof. Assume all sets and maps are implemented using hash tables. For a sample hyperedge e_i , computing $N_{e_i} \cup N_{e_j}$ for every $e_j \in N_{e_i}$ takes $O(\sum_{e_j \in N_{e_i}} (|N_{e_i} \cup N_{e_j}|))$ time, and by Lemma 2, computing $h(\{e_i, e_j, e_k\})$ for all considered h-motif instances takes $O(\min(|e_i|, |e_j|) \cdot \sum_{e_j \in N_{e_i}} |N_{e_i} \cup N_{e_j}|)$ time. Thus, from $|N_{e_i} \cup N_{e_j}| \leq |N_{e_i}| + |N_{e_j}|$, the time complexity for processing a sample e_i is

$$\begin{aligned}
& O(\min(|e_i|, |e_j|) \cdot \sum_{e_j \in N_{e_i}} (|N_{e_i}| + |N_{e_j}|)) \\
& = O(|e_i| \cdot |N_{e_i}|^2 + \sum_{e_j \in N_{e_i}} (|e_j| \cdot |N_{e_j}|)),
\end{aligned}$$

Algorithm 4: MoCHy-A⁺: Approximate H-motif Counting Based on Hyperwedge Sampling

Input : (1) input hypergraph: $G = (V, E)$
(2) projected graph: $\bar{G} = (E, \wedge, \omega)$
(3) number of samples: r

Output: estimated count of each h-motif t 's instances: $\hat{M}[t]$

```

1  $\hat{M} \leftarrow$  map whose default value is 0
2 for  $n \leftarrow 1 \dots r$  do
3    $\wedge_{ij} \leftarrow$  a uniformly random hyperwedge
4   for each hyperedge  $e_k \in (N_{e_i} \cup N_{e_j} \setminus \{e_i, e_j\})$  do
5      $\hat{M}[h(\{e_i, e_j, e_k\})] += 1$ 
6   end
7 end
8 for each h-motif  $t$  do
9   if  $17 \leq t \leq 22$  then ▷ open h-motifs
10     $\hat{M}[t] \leftarrow \hat{M}[t] \cdot \frac{|\wedge|}{2r}$ 
11  else ▷ closed h-motifs
12     $\hat{M}[t] \leftarrow \hat{M}[t] \cdot \frac{|\wedge|}{3r}$ 
13  end
14 end
15 return  $\hat{M}$ 

```

which can be written as

$$\begin{aligned}
& O(\sum_{e_i \in E} (\mathbb{1}(e_i \text{ is sampled}) \cdot |e_i| \cdot |N_{e_i}|^2) \\
& + \sum_{e_j \in E} (\mathbb{1}(e_j \text{ is adjacent to the sample}) \cdot |e_j| \cdot |N_{e_j}|)).
\end{aligned}$$

From this, linearity of expectation, $\mathbb{E}[\mathbb{1}(e_i \text{ is sampled})] = \frac{1}{|E|}$, and $\mathbb{E}[\mathbb{1}(e_j \text{ is adjacent to the sample})] = \frac{|N_{e_j}|}{|E|}$, the average time complexity per sample hyperedge becomes $O(\frac{1}{|E|} \sum_{e_i \in E} (|e_i| \cdot |N_{e_i}|^2))$. Hence, the total time complexity for processing s samples is $O(\frac{s}{|E|} \sum_{e_i \in E} (|e_i| \cdot |N_{e_i}|^2))$. \square

MoCHy-A⁺: Hyperwedge Sampling (Algorithm 4):

MoCHy-A⁺, which provides a better trade-off between speed and accuracy than MoCHy-A, is described in Algorithm 4. Different from MoCHy-A, which samples hyperedges, MoCHy-A⁺ is based on hyperwedge sampling. It selects r hyperwedges uniformly at random with replacement (line 4), and for each sampled hyperwedge $\wedge_{ij} \in \wedge$, it searches for all h-motif instances that contain \wedge_{ij} (lines 4-6). To this end, the hyperedges that are adjacent to e_i or e_j in the projected graph \bar{G} are considered (line 4). For each such instance $\{e_i, e_j, e_k\}$ of h-motif t , the corresponding estimate $\hat{M}[t]$ is incremented (line 5). Lastly, each estimate $\hat{M}[t]$ is rescaled so that it unbiasedly estimates $M[t]$, as formalized in Theorem 4. To this end, each estimate is multiplied by the reciprocal of the expected number of times that each instance of h-motif t is counted. Note that each instance of open and closed h-motifs contains 2 and 3 hyperwedges, respectively. Each instance of closed h-motifs is counted if one of the 3 hyperwedges in it is sampled, while that of open h-motifs is counted if one of the 2 hyperwedges in it is sampled. Thus, on average, each instance of open and closed h-motifs is counted $\frac{3r}{|\wedge|}$ and $\frac{2r}{|\wedge|}$ times, respectively.

Theorem 4 (Bias and Variance of MoCHy-A⁺). *For every h-motif t , Algorithm 4 provides an unbiased estimate $\hat{M}[t]$ of the count $M[t]$ of its instances, i.e.,*

$$\mathbb{E}[\hat{M}[t]] = M[t]. \quad (6)$$

For every closed motif t , the variance of the estimate is

$$\text{Var}[\hat{M}[t]] = \frac{1}{3r} \cdot M[t] \cdot (|\wedge| - 3) + \frac{1}{9r} \sum_{n=0}^1 q_n[t] \cdot (n|\wedge| - 9), \quad (7)$$

where $q_n[t]$ is the number of pairs of h-motif t 's instances that share n hyperwedges. For every open motif t , the variance is

$$\text{Var}[\hat{M}[t]] = \frac{1}{2r} \cdot M[t] \cdot (|\wedge| - 2) + \frac{1}{4r} \sum_{n=0}^1 q_n[t] \cdot (n|\wedge| - 4). \quad (8)$$

Proof. See Appendix B. \square

The time complexity of MoCHy-A⁺ is given in Theorem 5.

Theorem 5 (Complexity of MoCHy-A⁺). *The average time complexity of Algorithm 4 is $O(\frac{r}{|\wedge|} \sum_{e_i \in E} (|e_i| \cdot |N_{e_i}|^2))$.*

Proof. Assume all sets and maps are implemented using hash tables. For a sample hyperwedge \wedge_{ij} , computing $N_{e_i} \cup N_{e_j}$ takes $O(|N_{e_i} \cup N_{e_j}|)$ time, and by Lemma 2, computing $h(\{e_i, e_j, e_k\})$ for all considered h-motif instances takes $O(\min(|e_i|, |e_j|) \cdot |N_{e_i} \cup N_{e_j}|)$ time. Thus, from $|N_{e_i} \cup N_{e_j}| \leq |N_{e_i}| + |N_{e_j}|$, the time complexity for processing a sample \wedge_{ij} is $O(\min(|e_i|, |e_j|) \cdot (|N_{e_i}| + |N_{e_j}|)) = O(|e_i| \cdot |N_{e_i}| + |e_j| \cdot |N_{e_j}|)$, which can be written as

$$O\left(\sum_{e_i \in E} (\mathbb{1}(e_i \text{ is included in the sample}) \cdot |e_i| \cdot |N_{e_i}|) + \sum_{e_j \in E} (\mathbb{1}(e_j \text{ is included in the sample}) \cdot |e_j| \cdot |N_{e_j}|)\right).$$

From this, linearity of expectation, $\mathbb{E}[\mathbb{1}(e_i \text{ is included in the sample})] = \frac{|N_{e_i}|}{|\wedge|}$, and $\mathbb{E}[\mathbb{1}(e_j \text{ is included in the sample})] = \frac{|N_{e_j}|}{|\wedge|}$, the average time complexity per sample hyperwedge is $O(\frac{1}{|\wedge|} \sum_{e_i \in E} (|e_i| \cdot |N_{e_i}|^2))$. Hence, the total time complexity for processing r samples is $O(\frac{r}{|\wedge|} \sum_{e_i \in E} (|e_i| \cdot |N_{e_i}|^2))$. \square

Comparison of MoCHy-A and MoCHy-A⁺: Empirically, MoCHy-A⁺ provides a better trade-off between speed and accuracy than MoCHy-A, as presented in Section 5.4. Below, we provide an analysis that supports this observation.

Assume that the numbers of samples in both algorithms are set so that $\alpha = \frac{s}{|E|} = \frac{r}{|\wedge|}$. For each h-motif t , since both estimates $\bar{M}[t]$ of MoCHy-A and $\hat{M}[t]$ of MoCHy-A⁺ are unbiased (see Eq. (4) and (6)), we only need to compare their variances. By Eq. (5), $\text{Var}[\bar{M}[t]] = O(\frac{M[t] + p_1[t] + p_2[t]}{\alpha})$, and by Eq. (7) and Eq. (8), $\text{Var}[\hat{M}[t]] = O(\frac{M[t] + q_1[t]}{\alpha})$. By definition, $q_1[t] \leq p_2[t]$, and thus $\frac{M[t] + q_1[t]}{\alpha} \leq \frac{M[t] + p_1[t] + p_2[t]}{\alpha}$. Moreover, in real-world hypergraphs, $p_1[t]$ tends to be several orders of magnitude larger than the other terms (i.e., $p_2[t]$, $q_1[t]$, and $M[t]$), and thus $\bar{M}[t]$ of MoCHy-A tends to have much larger variance (and thus much larger estimation error) than $\hat{M}[t]$ of MoCHy-A⁺. Despite this fact, MoCHy-A and MoCHy-A⁺ have the same time complexity, which is $O(\alpha \cdot \sum_{e_i \in E} (|e_i| \cdot |N_{e_i}|^2))$ (see Theorems 3 and 5). Hence,

MoCHy-A⁺ is expected to provide a better trade-off between speed and accuracy than MoCHy-A, as confirmed empirically in Section 5.4.

4.4 Parallel and On-the-fly Implementations

We discuss parallelization of MoCHy and then on-the-fly computation of projected graphs.

Parallelization: All versions of MoCHy and hypergraph projection are easily parallelized. Specifically, we can parallelize hypergraph projection and MoCHy-E by letting multiple threads process different hyperedges (in line 3 of Algorithm 1 and line 2 Algorithm 2, respectively) independently in parallel. Similarly, we can parallelize MoCHy-A and MoCHy-A⁺ by letting multiple threads sample and process different hyperedges (in line 3 of Algorithm 3) and hyperwedges (in line 3 of Algorithm 4), respectively, independently in parallel. The estimated counts of the same h-motif obtained by different threads are summed up only once before they are returned as outputs. We present some empirical results in Section 5.4.

H-motif Counting without Projected Graphs: If the input hypergraph G is large, computing its projected graph \bar{G} (Algorithm 3) is time and space consuming. Specifically, building \bar{G} takes $O(\sum_{\wedge_{ij} \in \wedge} |e_i \cap e_j|)$ time (see Lemma 1) and requires $O(|E| + |\wedge|)$ space, which often exceeds $O(\sum_{e_i \in E} |e_i|)$ space required for storing G . Thus, instead of precomputing \bar{G} entirely, we can build it incrementally while memoizing partial results within a given memory budget. For example, in MoCHy-A⁺ (Algorithm 4), we compute the neighborhood of a hyperedge $e_i \in E$ in \bar{G} (i.e., $\{(k, \omega(\wedge_{ik})) : k \in N_{e_i}\}$) only if (1) a hyperwedge with e_i (e.g., \wedge_{ij}) is sampled (in line 3) and (2) its neighborhood is not memoized.

This incremental computation of \bar{G} can be beneficial in terms of speed since it skips projecting the neighborhood of a hyperedge if no hyperwedges containing it is sampled. However, it can also be harmful if memoized results exceed the memory budget and some parts of \bar{G} need to be rebuilt multiple times. Then, given a memory budget in bits, how should we prioritize hyperedges if all their neighborhoods cannot be memoized? According to our experiments, despite their large size, memoizing the neighborhoods of hyperedges with high degree in \bar{G} makes MoCHy-A⁺ faster than memoizing the neighborhoods of randomly chosen hyperedges or least recently used (LRU) hyperedges. In Section 5.4, we experimentally examine the effects of the memory budget on the speed of MoCHy-A⁺.

5. EXPERIMENTS

In this section, we review our experiments that we design for answering the following questions:

- **Q1. Comparison with Random:** Does counting instances of different h-motifs reveal structural design principles of real-world hypergraphs distinguished from those of random hypergraphs?
- **Q2. Comparison across Domains:** Do characteristic profiles capture local structural patterns of hypergraphs unique to each domain?
- **Q3. Performance of Counting Algorithms:** How fast and accurate are the different versions of MoCHy? Does the advanced version outperform the basic ones?

Table 2: Real-world and random hypergraphs have distinct distributions of h-motif instances. We report the absolute number of each h-motif’s instances in a real-world hypergraph from each domain and its corresponding random hypergraph. The counts are ranked, and the ranks in the real-world and corresponding random hypergraphs are compared.

h-motif	coauth-DBLP			contact-primary			email-EU			tags-math			threads-math		
	real	randomized	rank	real	randomized	rank	real	randomized	rank	real	randomized	rank	real	randomized	rank
	count (rank)	count (rank)	diff	count (rank)	count (rank)	diff	count (rank)	count (rank)	diff	count (rank)	count (rank)	diff	count (rank)	count (rank)	diff
1	9.7E+07 (7)	1.3E+09 (4)	3	4.8E+04 (16)	2.8E+07 (5)	11	7.5E+06 (13)	1.7E+08 (7)	6	9.3E+08 (13)	2.2E+11 (6)	7	6.5E+08 (7)	2.4E+11 (4)	3
2	7.0E+09 (2)	7.2E+09 (2)	0	1.1E+08 (3)	8.6E+07 (3)	0	6.3E+08 (2)	8.2E+08 (3)	1	1.6E+12 (2)	1.6E+12 (2)	0	1.1E+12 (2)	7.7E+11 (2)	0
3	2.2E+06 (17)	6.8E+03 (14)	3	2.8E+03 (21)	1.7E+05 (16)	5	1.6E+06 (21)	7.8E+05 (17)	4	3.0E+06 (20)	1.1E+09 (15)	5	1.7E+05 (20)	1.7E+08 (14)	6
4	9.7E+06 (11)	1.0E+05 (12)	1	8.4E+02 (24)	9.2E+05 (12)	12	4.3E+06 (16)	1.5E+07 (12)	4	1.5E+08 (17)	1.6E+10 (12)	5	3.3E+06 (13)	1.2E+09 (11)	2
5	1.5E+08 (6)	1.1E+05 (11)	5	4.6E+06 (5)	1.6E+06 (11)	6	7.5E+07 (7)	1.1E+07 (13)	6	7.5E+09 (8)	2.5E+10 (8)	0	4.1E+08 (8)	1.7E+09 (10)	2
6	9.9E+08 (3)	1.7E+06 (9)	6	1.3E+07 (4)	8.2E+06 (7)	3	3.9E+08 (4)	1.9E+08 (6)	2	6.8E+11 (3)	3.3E+11 (4)	1	1.4E+10 (4)	1.1E+10 (8)	4
7	1.9E+05 (23)	0.0E+00 (21)	2	1.6E+04 (17)	2.0E+02 (24)	7	7.5E+04 (24)	1.2E+02 (25)	1	8.4E+05 (25)	9.2E+05 (25)	0	8.5E+03 (24)	1.7E+04 (24)	0
8	3.9E+05 (22)	9.4E-01 (20)	2	4.6E+03 (20)	2.6E+03 (22)	2	4.2E+06 (17)	2.5E+04 (21)	4	2.0E+06 (23)	3.4E+07 (22)	1	2.2E+04 (23)	3.5E+05 (21)	2
9	2.4E+06 (16)	0.0E+00 (21)	5	1.7E+05 (12)	4.6E+03 (20)	8	1.8E+06 (20)	1.1E+04 (22)	2	1.4E+08 (18)	5.4E+07 (21)	3	4.8E+05 (17)	4.6E+05 (20)	3
10	7.5E+06 (13)	1.2E+01 (18)	5	5.7E+04 (15)	5.5E+04 (17)	2	2.8E+07 (10)	1.7E+06 (14)	4	7.1E+08 (14)	1.9E+09 (14)	0	2.3E+06 (15)	9.3E+06 (17)	2
11	8.6E+06 (12)	3.7E+00 (19)	7	4.1E+05 (11)	2.4E+04 (18)	7	9.0E+06 (11)	1.9E+05 (19)	8	3.6E+09 (10)	7.5E+08 (16)	6	2.9E+06 (14)	3.1E+06 (18)	4
12	6.4E+07 (8)	1.8E+02 (16)	8	1.7E+05 (13)	2.7E+05 (14)	1	8.2E+07 (6)	2.4E+07 (10)	4	6.9E+10 (6)	2.4E+10 (10)	4	8.2E+07 (10)	6.2E+07 (15)	5
13	1.6E+04 (26)	0.0E+00 (21)	5	5.5E+03 (19)	1.6E+00 (26)	7	2.7E+04 (26)	4.0E-01 (26)	0	1.1E+06 (24)	1.6E+04 (26)	2	1.3E+02 (26)	0.0E+00 (26)	0
14	1.4E+05 (24)	0.0E+00 (21)	3	6.0E+03 (18)	7.1E+01 (25)	7	7.2E+05 (22)	3.7E+02 (24)	2	2.8E+07 (19)	1.8E+06 (24)	5	4.6E+03 (25)	9.8E+02 (25)	0
15	6.5E+05 (19)	0.0E+00 (21)	2	1.7E+03 (22)	8.6E+02 (23)	1	3.6E+06 (19)	5.0E+04 (20)	1	2.9E+08 (15)	5.7E+07 (20)	5	2.9E+04 (22)	2.0E+04 (23)	1
16	2.0E+06 (18)	0.0E+00 (21)	3	1.4E+02 (25)	3.2E+03 (21)	4	6.7E+06 (14)	1.7E+06 (15)	1	1.9E+09 (11)	5.8E+08 (18)	7	2.4E+05 (18)	1.3E+05 (22)	4
17	4.2E+05 (21)	2.0E+06 (8)	13	1.0E+03 (23)	6.3E+05 (13)	10	3.8E+04 (25)	7.7E+05 (16)	9	5.2E+05 (26)	5.0E+08 (19)	7	2.3E+05 (19)	9.3E+08 (12)	7
18	2.6E+06 (15)	6.4E+07 (7)	8	1.2E+02 (26)	7.0E+06 (8)	18	6.0E+06 (15)	4.0E+07 (8)	7	2.5E+06 (22)	1.6E+10 (13)	9	8.2E+05 (16)	1.3E+10 (7)	9
19	3.6E+07 (9)	6.7E+07 (6)	3	2.0E+06 (6)	1.2E+07 (6)	0	8.7E+06 (12)	2.9E+07 (9)	3	9.3E+08 (12)	2.4E+10 (9)	3	3.5E+08 (9)	1.8E+10 (6)	3
20	3.4E+08 (5)	2.2E+09 (3)	2	6.0E+05 (10)	1.3E+08 (2)	8	2.2E+08 (5)	1.2E+09 (2)	3	9.2E+09 (7)	7.2E+11 (3)	4	2.0E+09 (5)	2.4E+11 (3)	2
21	8.0E+08 (4)	5.6E+08 (5)	1	1.7E+08 (2)	5.7E+07 (4)	2	5.3E+08 (3)	2.3E+08 (4)	1	1.2E+11 (5)	2.8E+11 (5)	0	2.8E+10 (3)	8.6E+10 (5)	2
22	1.7E+10 (1)	1.8E+10 (1)	0	3.1E+08 (1)	5.8E+08 (1)	0	4.9E+09 (1)	8.5E+09 (1)	0	6.6E+12 (1)	7.6E+12 (1)	0	1.1E+12 (1)	1.2E+12 (1)	0
23	2.5E+04 (25)	1.3E+01 (17)	8	1.2E+05 (14)	5.4E+03 (19)	5	8.8E+04 (23)	4.0E+03 (23)	0	2.5E+06 (21)	7.9E+06 (23)	2	1.4E+05 (21)	7.7E+05 (19)	2
24	4.5E+05 (20)	1.5E+03 (15)	5	7.7E+05 (9)	1.8E+05 (15)	6	4.2E+06 (18)	5.4E+05 (18)	0	2.2E+08 (16)	7.2E+08 (17)	1	7.6E+06 (12)	3.1E+07 (16)	4
25	3.9E+06 (14)	4.7E+04 (13)	1	1.7E+06 (8)	1.8E+06 (10)	2	3.2E+07 (9)	2.0E+07 (11)	2	6.0E+09 (9)	2.0E+10 (11)	2	8.0E+07 (11)	4.2E+08 (13)	2
26	2.3E+07 (10)	4.9E+05 (10)	0	1.8E+06 (7)	6.1E+06 (9)	2	7.5E+07 (8)	2.1E+08 (5)	3	1.3E+11 (4)	1.8E+11 (7)	3	1.2E+09 (6)	1.9E+09 (9)	3

Table 3: Statistics of 11 real hypergraphs from 5 domains.

Dataset	V	E	\wedge	# h-motifs
coauth-DBLP	1,924,991	2,466,792	125M	26.3B \pm 18M
coauth-geology	1,256,385	1,203,895	37.6M	6B \pm 4.8M
coauth-history	1,014,734	895,439	1.7M	83.2M
contact-primary	242	12,704	2.2M	617M
contact-high	327	7,818	593K	69.7M
email-Enron	143	1,512	87.8K	9.6M
email-EU	998	25,027	8.3M	7B
tags-ubuntu	3,029	147,222	564M	4.3T \pm 1.5B
tags-math	1,629	170,476	913M	9.2T \pm 3.2B
threads-ubuntu	125,602	166,999	21.6M	11.4B
threads-math	176,445	595,749	647M	2.2T \pm 883M

5.1 Experimental Settings

Machines: We conducted all the experiments on a machine with an AMD Ryzen 9 3900X CPU and 128GB RAM.

Implementations: We implemented every version of MoChy using C++ and OpenMP.

Datasets: We used the following 11 real-world hypergraphs from five different domains:

- **co-authorship** (coauth-DBLP, coauth-geology [53], and coauth-history [53]): A node represents an author. A hyperedge represents the authors of a publication.
- **contact** (contact-primary [54] and contact-high [40]): A node represents a person. A hyperedge represents a group interaction among individuals.
- **email** (email-Enron [32] and email-EU [35, 62]): A node represents an e-mail account. A hyperedge consists of the sender and all receivers of an email.
- **tags** (tags-ubuntu and tags-math): A node represents a tag. A hyperedge represents the tags attached to a post.

- **threads** (threads-ubuntu and threads-math): A node represents a user. A hyperedge groups all users participating in a thread.

These hypergraphs are made public by the authors of [10]¹, and in Table 3 we provide some statistics of the hypergraphs after removing duplicated hyperedges. We used MoChy-E for the *coauth-history* dataset, the *threads-ubuntu* dataset, and all datasets from the **contact** and **email** domains. For the other datasets, we used MoChy-A⁺ with $r = 2,000,000$, unless otherwise stated. For the *tags-ubuntu*, *tags-math*, and *threads-math* datasets with trillions of h-motifs, we set the memory budget to 0.8% of the edges in the projected graphs, as described in Section 4.4, while we precomputed the projected graphs for the other datasets. We used a single thread unless otherwise stated. We computed CPs based on five hypergraphs randomized as described in Section 3.2.

5.2 Q1. Comparison with Random

To answer Q1, we analyze the counts of different h-motifs’ instances in real and random hypergraphs. In Table 2, we report the (approximated) count of each h-motif t ’s instances in each real hypergraph with the corresponding count averaged over five random hypergraphs that are obtained as described in Section 3.2. We rank h-motifs by the counts of their instances and examine the difference between the ranks in real and corresponding random hypergraphs. As seen in the table, the count distributions in real hypergraphs are clearly distinguished from those of random hypergraphs.

H-motifs in Random Hypergraphs: We first notice from Table 2 that instances of h-motifs 17 and 18 appear much more frequently in random hypergraphs than in real hypergraphs from all domains. For example, instances of h-motif 17 appear only about 520 thousand times in the *tags-math dataset*, while they appeared about 500 million times (about

¹<https://www.cs.cornell.edu/~arb/data/>

960 \times more often) in the corresponding randomized hypergraphs. Additionally, in the *threads-math* dataset, instances of h-motif 18 appear about 824 thousand times, while they appear about 13 billion times (about 15,400 \times more often). Instances of h-motifs 17 and 18 consist of a hyperedge and its two disjoint subsets (see Figure 4).

H-motifs in Co-authorship Hypergraphs: We observe that instances of h-motifs 10, 11 and 12 appear more frequently in all three hypergraphs from the **co-authorship** domain than in the corresponding random hypergraphs. For example, while there is no single instance of h-motif 12 in the corresponding random hypergraphs, there are about 400 thousand such instances in the *coauth-history* dataset. While there are only about 180 instances of h-motif 12 in the corresponding random hypergraphs, there are about 64 million such instances (about 356,000 \times more instances) in the *coauth-history* dataset. As seen in Figure 4, in instances of h-motifs 10, 11, and 12, a hyperedge is overlapped with the two other overlapped hyperedges in three different ways.

H-motifs in Contact Hypergraphs: Instances of h-motifs 9, 13, and 14 are noticeably more common in both **contact** datasets than in the corresponding random hypergraphs. As seen in Figure 4, in instances of h-motifs 9, 13 and 14, hyperedges are tightly connected and nodes are mainly located in the intersections of all or some hyperedges.

H-motifs in Email Hypergraphs: Both email datasets contain particularly many instances of h-motifs 8 and 10, compared to the corresponding random hypergraphs. As seen in Figure 4, instances of h-motifs 8 and 10 consist of three hyperedges where most nodes are contained in one hyperedge.

H-motifs in Tags Hypergraphs: In addition to instances of h-motif 11, which are common in most real hypergraphs, instances of h-motif 16, where all seven regions are not empty (see Figure 4), particularly frequent in both **tags** datasets than in corresponding random hypergraphs.

H-motifs in Threads Hypergraphs: Lastly, in both datasets from the **threads** domain, instances of h-motifs 12 and 24 are noticeably more frequent than expected from the corresponding random hypergraphs.

5.3 Q2. Comparison across Domains

To answer **Q2**, we compare the characteristic profiles (CPs) of the real-world hypergraphs. In Figure 6, we present the CPs (i.e., the significances of the 26 h-motifs) of each hypergraph. As seen in the figure, hypergraphs from the same domains have similar CPs. Specifically, all three hypergraphs from the **co-authorship** domain share extremely similar CPs, even when the absolute counts of h-motifs in them are several orders of magnitude different. Similarly, the CPs of both hypergraphs from the **tags** domain are extremely similar. However, the CPs of the hypergraphs from the **co-authorship** domain are clearly distinguished by them of the hypergraphs from the **tags** domain. While the CPs of the hypergraphs from the **contact** domain and the CPs of those from the **email** domain are similar for the most part, they are distinguished by the significance of h-motif 3. These observations confirm that CPs accurately capture local structural patterns of real-world hypergraphs.

To further verify the effectiveness of CPs based on h-motifs, we compare them with CPs based on network mo-

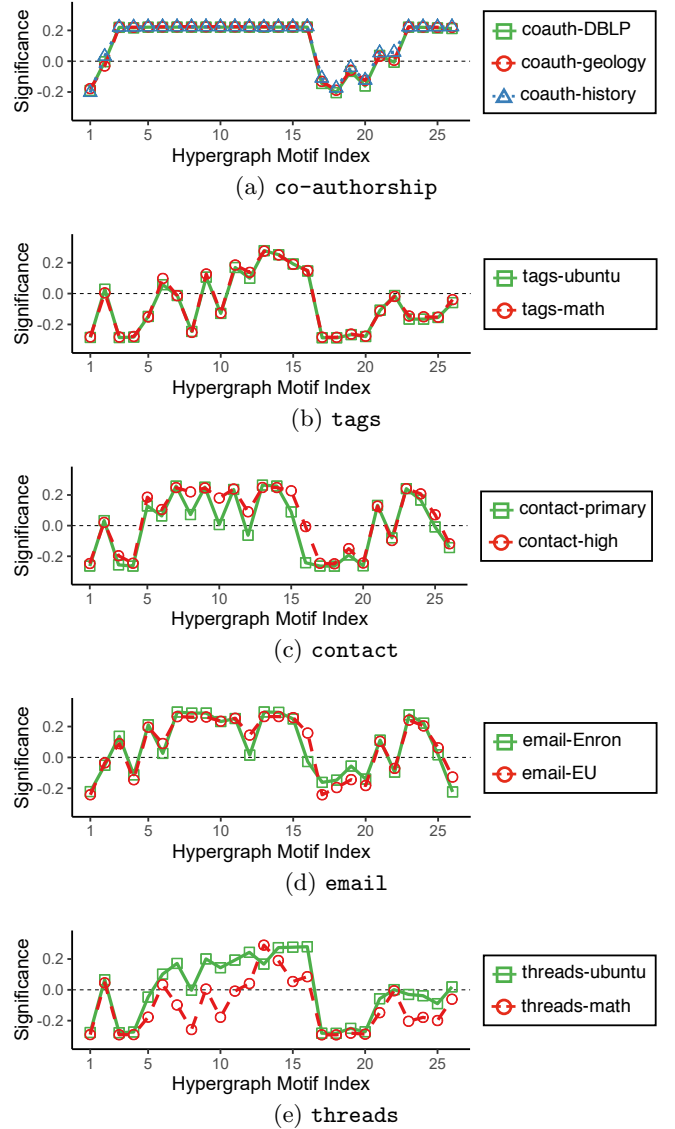
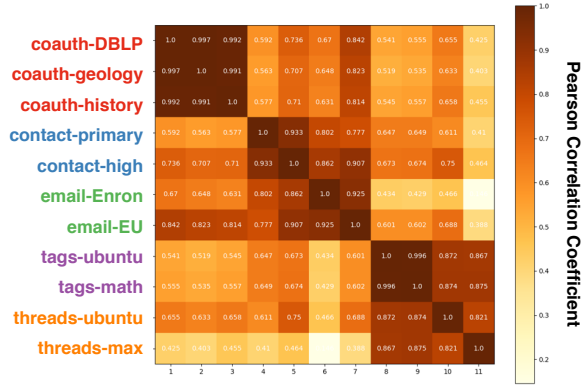


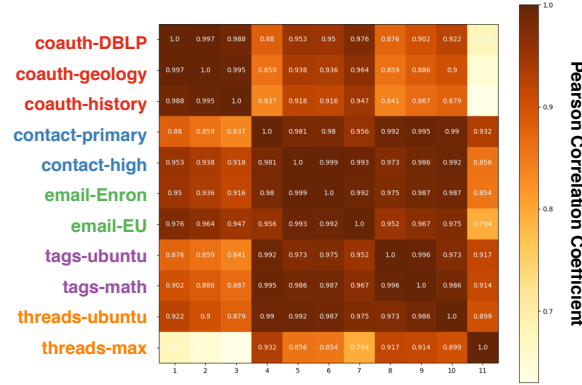
Figure 6: Characteristic profiles (CPs) capture local structural patterns in real-world hypergraphs accurately. The CPs are similar within domains but different across domains. Note that the significance of h-motif 3 distinguishes the **contact** hypergraphs from the **email** hypergraphs.

tifs. Specifically, we represent each hypergraph $G = (V, E)$ as a bipartite graph $G' = (V', E')$ where $V' := V \cup E$ and $E' := \{(v, e) \in V \times E : v \in e\}$. That is, the two types of nodes in the transformed bipartite graph G' represent the nodes and hyperedges, resp., in the original hypergraph G , and each edge (v, e) in G' indicates that the node v belongs to the hyperedge e in G . Then, we compute the CPs based on the network motifs consisting of 3 to 5 nodes². Lastly, based on both CPs, we compute the similarity matrices (specifically, correlation coefficient matrices) of the real-world hypergraphs. As seen in Figure 7, the domains of the real-world hypergraphs are distinguished more clearly by the CPs based on h-motifs than by the CPs based on network motifs. Numerically, when the CPs based on h-motifs are used, the average correlation coefficient is 0.93 within

²We used Motivo [14], which is a state-of-the-art approximate algorithm for network motif counting.



(a) Similarity Matrix from Hypergraph Motifs (Proposed)



(b) Similarity Matrix from Network Motifs (Baseline)

Figure 7: Characteristic profiles (CPs) based on hypergraph motifs (h-motifs) capture local structural patterns more accurately than CPs based on network motifs. The CPs based on h-motifs clearly distinguishes the domains of the real-world hypergraphs (the average correlation coefficient is 0.93 within domains and 0.63 across domains), compared to the CPs based on network motifs (the average correlation coefficient is 0.97 within domains and 0.92 across domains).

domains and 0.63 across domains, and thus the gap is 0.3. However, when the CPs based on network motifs are used, the average correlation coefficient is 0.97 within domains and 0.92 across domains, and thus the gap is just 0.05. These results support that h-motifs play a key role in capturing the local structural patterns of real-world hypergraphs.

5.4 Q3. Performance of Counting Algorithms

To answer Q3, we test the speed and accuracy of all versions of MoChy under various settings. To this end, we measure elapsed time and relative error defined as

$$\frac{\sum_{t=1}^{26} |M[t] - \bar{M}[t]|}{\sum_{t=1}^{26} M[t]} \text{ and } \frac{\sum_{t=1}^{26} |M[t] - \hat{M}[t]|}{\sum_{t=1}^{26} M[t]},$$

for MoChy-A and MoChy-A⁺, respectively.

Speed and Accuracy: In Figure 8, we report the elapsed time and relative error of all versions of MoChy on the 6 different datasets where MoChy-E terminates within a reasonable time. The numbers of samples in MoChy-A and MoChy-A⁺ are set to $\{2.5 \times k : 1 \leq k \leq 10\}$ percent of the counts of hyperedges and hyperwedges, respectively. As seen in the figure, MoChy-A⁺ provides the best trade-off between speed and accuracy. For example, in the *threads-*

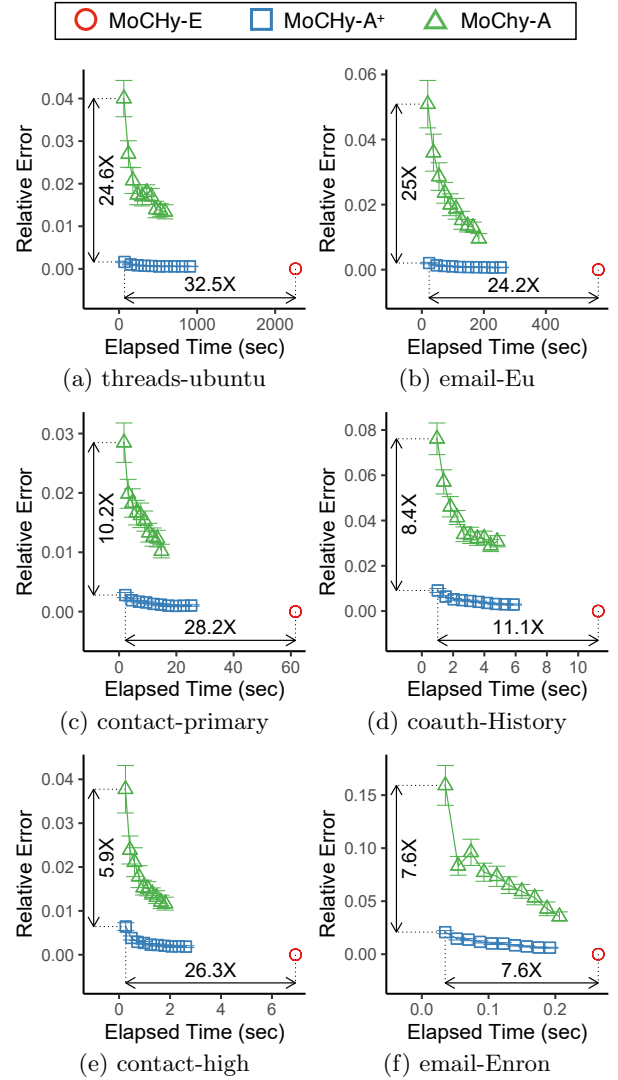


Figure 8: MoChy-A⁺ provides the best trade-off between speed and accuracy. Specifically, MoChy-A⁺ produces up to 25× more accurate estimation than MoChy-A, and it is up to 32.5× faster than MoChy-E. The error bars indicate ± 1 standard error over 20 trials.

ubuntu dataset, MoChy-A⁺ provides 24.6× lower relative error than MoChy-A, consistently with our theoretical analysis (see the last paragraph of Section 4.3). Moreover, in the same dataset, MoChy-A⁺ is 32.5× faster than MoChy-E with little sacrifice on accuracy.

Effects of the Sample Size on CPs: In Figure 9, we report the CPs obtained by MoChy-A⁺ with different numbers of hyperwedge samples on 3 datasets. Even with a smaller number of samples, the CPs are estimated near perfectly.

Parallelization: In Figure 10, we measure the running times of MoChy-E and MoChy-A⁺ with different numbers of threads on the *threads-ubuntu* dataset. As seen in the figure, both algorithms achieve significant speedups with multiple threads. Specifically, with 8 threads, MoChy-E and MoChy-A⁺ ($r = 1M$) achieve speedups of 5.4 and 6.7, respectively.

Effects of On-the-fly Computation on Speed: We analyze the effects of the on-the-fly computation of projected graphs (discussed in Section 4.4) on the speed of MoChy-A⁺

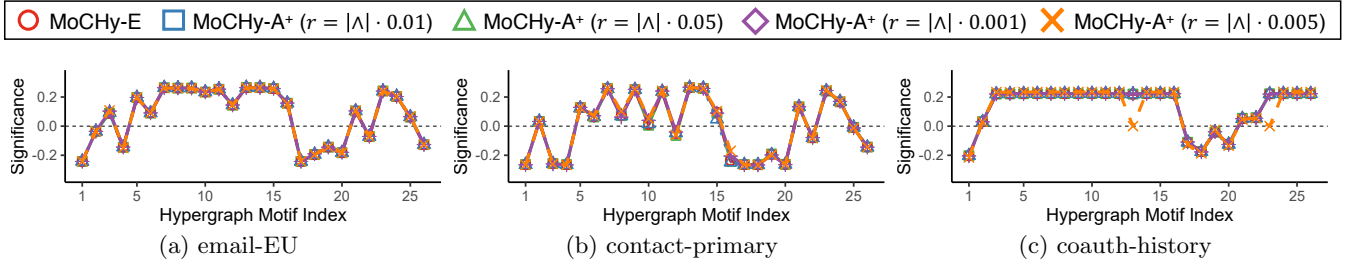


Figure 9: Using MoChy-A⁺, characteristic profiles (CPs) can be estimated accurately from a small number of samples.

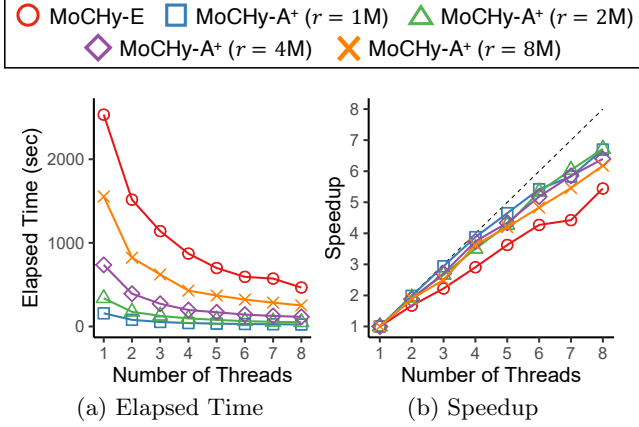


Figure 10: Both MoChy-E and MoChy-A⁺ achieve significant speedups with multiple threads.

under different memory budgets for memoization. To this end, we use the *threads-ubuntu* dataset, and we set the memory budgets so that up to $\{0\%, 0.1\%, 1\%, 10\%, 100\%\}$ of the edges in the projected graph can be memoized. The results are shown in Figure 11. As the memory budget increases, MoChy-A⁺ becomes faster, avoiding repeated computation. Due to our careful prioritization scheme based on degree, by memoizing only 1% of the edges, MoChy-A⁺ achieves speedups of about 2.

6. CONCLUSIONS

In this work, we introduce hypergraph motifs (h-motifs), and using them, we investigate the local structures of 11 real-world hypergraphs from 5 different domains. We summarize our contributions as follows:

- **Novel Concepts:** We define 26 h-motifs, which describe connectivity patterns of 3 connected hyperedges in a unique and exhaustive way, independently of the sizes of hyperedges (Figure 4).
- **Fast and Provable Algorithms:** We propose 3 parallel algorithms for (approximately) counting every h-motif's instances, and we theoretically and empirically analyze their speed and accuracy. Both approximate algorithms yield unbiased estimates (Theorems 2 and 4), and especially the advanced one is up to $32\times$ faster than the exact algorithm, with little sacrifice on accuracy (Figure 8).
- **Discoveries in 11 Real-world Hypergraphs:** We confirm the efficacy of h-motifs by showing that local structural patterns captured by them are similar within domains but different across domains (Figures 6 and 7).

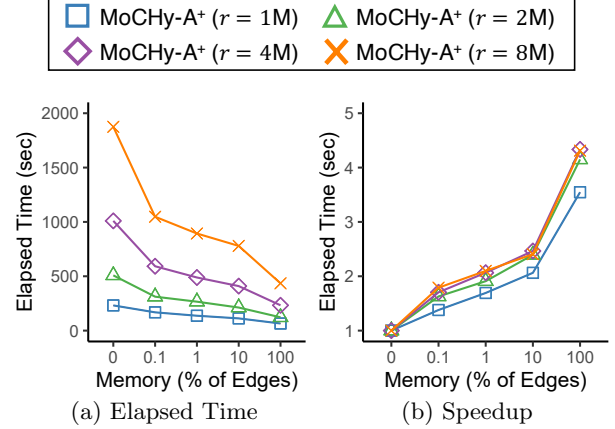


Figure 11: Memoizing a small fraction of projected graphs leads to significant speedups of MoChy-A⁺.

Future research directions include (1) extending h-motifs to richer hypergraphs, such as heterogeneous or temporal hypergraphs, and (2) incorporating h-motifs into various tasks, such as hypergraph embedding, ranking, and clustering.

APPENDIX

A. PROOF OF THEOREM 2

We let $X_{ij}[t]$ be a random variable indicating whether the i -th sampled hyperedge (in line 3 of Algorithm 3) is included in the j -th instance of h-motif t or not. That is, $X_{ij}[t] = 1$ if the hyperedge is included in the instance, and $X_{ij}[t] = 0$ otherwise. We let $\bar{m}[t]$ be the number of times that h-motif t 's instances are counted while processing s sampled hyperedges. That is,

$$\bar{m}[t] := \sum_{i=1}^s \sum_{j=1}^{M[t]} X_{ij}[t]. \quad (9)$$

Then, by lines 10-12 of Algorithm 3,

$$\bar{M}[t] = \bar{m}[t] \cdot \frac{|E|}{3s}. \quad (10)$$

Proof of the Bias of $\bar{M}[t]$ (Eq. (4)):

Proof. Since each h-motif instance contains three hyperedges, the probability that each i -th sampled hyperedge is contained in each j -th instance of h-motif t is

$$P[X_{ij}[t] = 1] = \mathbb{E}[X_{ij}[t]] = \frac{3}{|E|}. \quad (11)$$

From linearity of expectation,

$$\mathbb{E}[\bar{m}[t]] = \sum_{i=1}^s \sum_{j=1}^{M[t]} \mathbb{E}[X_{ij}[t]] = \sum_{i=1}^s \sum_{j=1}^{M[t]} \frac{3}{|E|} = \frac{3s \cdot M[t]}{|E|}.$$

Then, by Eq. (10), $\mathbb{E}[\bar{M}[t]] = \frac{|E|}{3s} \cdot \mathbb{E}[\bar{m}[t]] = M[t]$. \square

Proof of the Variance of $\bar{M}[t]$ (Eq. (5)):

Proof. From Eq. (11) and $X_{ij}[t] = X_{ij}[t]^2$, the variance of each random variable $X_{ij}[t]$ is

$$\text{Var}[X_{ij}[t]] = \mathbb{E}[X_{ij}[t]^2] - \mathbb{E}[X_{ij}[t]]^2 = \frac{3}{|E|} - \frac{9}{|E|^2}. \quad (12)$$

Consider the covariance between $X_{ij}[t]$ and $X_{i'j'}[t]$. If $i = i'$, then from Eq. (11),

$$\begin{aligned} \text{Cov}(X_{ij}[t], X_{i'j'}[t]) &= \mathbb{E}[X_{ij}[t] \cdot X_{i'j'}[t]] - \mathbb{E}[X_{ij}[t]]\mathbb{E}[X_{i'j'}[t]] \\ &= P[X_{ij}[t] = 1, X_{i'j'}[t] = 1] - \mathbb{E}[X_{ij}[t]]\mathbb{E}[X_{i'j'}[t]] \\ &= P[X_{ij}[t] = 1] \cdot P[X_{i'j'}[t] = 1 | X_{ij}[t] = 1] - \mathbb{E}[X_{ij}[t]]\mathbb{E}[X_{i'j'}[t]] \\ &= \frac{3}{|E|} \cdot \frac{l_{jj'}}{3} - \frac{9}{|E|^2} = \frac{l_{jj'}}{|E|} - \frac{9}{|E|^2}, \end{aligned} \quad (13)$$

where $l_{jj'}$ is the number of hyperedges that the j -th and j' -th instances share. However, since hyperedges are sampled independently (specifically, uniformly at random with replacement), if $i \neq i'$, then $\text{Cov}(X_{ij}[t], X_{i'j'}[t]) = 0$. This observation, Eq. (9), Eq. (12), and Eq. (13) imply

$$\begin{aligned} \text{Var}[\bar{m}[t]] &= \text{Var}\left[\sum_{i=1}^s \sum_{j=1}^{M[t]} X_{ij}[t]\right] \\ &= \sum_{i=1}^s \sum_{j=1}^{M[t]} \text{Var}[X_{ij}[t]] + \sum_{i=1}^s \sum_{j \neq j'} \text{Cov}(X_{ij}[t], X_{ij'}[t]) \\ &= s \cdot M[t] \cdot \left(\frac{3}{|E|} - \frac{9}{|E|^2}\right) + s \sum_{l=0}^2 p_l[t] \left(\frac{l}{|E|} - \frac{9}{|E|^2}\right), \end{aligned}$$

where $p_l[t]$ is the number of pairs of h-motif t 's instances that share l hyperedges. This and Eq. (10) imply Eq. (5). \square

B. PROOF OF THEOREM 4

A random variable $Y_{ij}[t]$ denotes whether the i -th sampled hyperwedge (in line 3 of Algorithm 4) is included in the j -th instance of h-motif t . That is, $Y_{ij}[t] = 1$ if the sampled hyperwedge is included in the instance, and $Y_{ij}[t] = 0$ otherwise. We let $\hat{m}[t]$ be the number of times that h-motif t 's instances are counted while processing r sampled hyperwedges. That is,

$$\hat{m}[t] := \sum_{i=1}^r \sum_{j=1}^{M[t]} Y_{ij}[t] \quad (14)$$

We use $w[t]$ to denote the number of hyperwedges included in each instance of h-motif t . That is,

$$w[t] := \begin{cases} 2 & \text{if h-motif } t \text{ is open,} \\ 3 & \text{if h-motif } t \text{ is closed.} \end{cases} \quad (15)$$

Then, by lines 8-14 of Algorithm 4,

$$\hat{M}[t] = \hat{m}[t] \cdot \frac{1}{w[t]} \cdot \frac{|\Lambda|}{r}. \quad (16)$$

Proof of the Bias of $\hat{M}[t]$ (Eq. (6)):

Proof. Since each instance of h-motif t contains $w[t]$ hyperwedges, the probability that each i -th sampled hyperwedge is contained in each j -th instance of h-motif t is

$$P[Y_{ij}[t] = 1] = \frac{w[t]}{|\Lambda|}. \quad (17)$$

From linearity of expectation,

$$\mathbb{E}[\hat{m}[t]] = \sum_{i=1}^r \sum_{j=1}^{M[t]} \mathbb{E}[Y_{ij}[t]] = \sum_{i=1}^r \sum_{j=1}^{M[t]} \frac{w[t]}{|\Lambda|} = \frac{w[t] \cdot r \cdot M[t]}{|\Lambda|}.$$

Then, by Eq. (16), $\mathbb{E}[\hat{M}[t]] = \mathbb{E}[\hat{m}[t]] \cdot \frac{1}{w[t]} \cdot \frac{|\Lambda|}{r} = M[t]$. \square

Proof of the Variance of $\hat{M}[t]$ (Eq. (7) and Eq. (8)):

Proof. From Eq. (17) and $Y_{ij}[t] = Y_{ij}[t]^2$, the variance of each random variable $Y_{ij}[t]$ is

$$\text{Var}[Y_{ij}[t]] = \mathbb{E}[Y_{ij}[t]^2] - \mathbb{E}[Y_{ij}[t]]^2 = \frac{w[t]}{|\Lambda|} - \frac{w[t]^2}{|\Lambda|^2}. \quad (18)$$

Consider the covariance between $Y_{ij}[t]$ and $Y_{i'j'}[t]$. If $i = i'$, then from Eq. (17),

$$\begin{aligned} \text{Cov}(Y_{ij}[t], Y_{i'j'}[t]) &= \mathbb{E}[Y_{ij}[t] \cdot Y_{i'j'}[t]] - \mathbb{E}[Y_{ij}[t]]\mathbb{E}[Y_{i'j'}[t]] \\ &= P[Y_{ij}[t] = 1, Y_{i'j'}[t] = 1] - \mathbb{E}[Y_{ij}[t]]\mathbb{E}[Y_{i'j'}[t]] \\ &= P[Y_{ij}[t] = 1] \cdot P[Y_{i'j'}[t] = 1 | Y_{ij}[t] = 1] - \mathbb{E}[Y_{ij}[t]]\mathbb{E}[Y_{i'j'}[t]] \\ &= \frac{w[t]}{|\Lambda|} \cdot \frac{n_{jj'}}{w[t]} - \frac{w[t]^2}{|\Lambda|^2} = \frac{n_{jj'}}{|\Lambda|} - \frac{w[t]^2}{|\Lambda|^2}, \end{aligned} \quad (19)$$

where $n_{jj'}$ is the number of hyperwedges that the j -th and j' -th instances share. However, since hyperwedges are sampled independently (specifically, uniformly at random with replacement), if $i \neq i'$, then $\text{Cov}(Y_{ij}[t], Y_{i'j'}[t]) = 0$. This observation, Eq. (14), Eq. (18), and Eq. (19) imply

$$\begin{aligned} \text{Var}[\hat{m}[t]] &= \text{Var}\left[\sum_{i=1}^r \sum_{j=1}^{M[t]} Y_{ij}[t]\right] \\ &= \sum_{i=1}^r \sum_{j=1}^{M[t]} \text{Var}[Y_{ij}[t]] + \sum_{i=1}^r \sum_{j \neq j'} \text{Cov}(Y_{ij}[t], Y_{ij'}[t]) \\ &= r \cdot M[t] \cdot \left(\frac{w[t]}{|\Lambda|} - \frac{w[t]^2}{|\Lambda|^2}\right) + r \sum_{n=0}^1 q_n[t] \cdot \left(\frac{n}{|\Lambda|} - \frac{w[t]^2}{|\Lambda|^2}\right), \end{aligned}$$

where $q_n[t]$ is the number of pairs of h-motif t 's instances that share n hyperwedges. This and Eq. (16) imply Eq. (7) and Eq. (8). \square

C. REFERENCES

- [1] S. Agarwal, J. Lim, L. Zelnik-Manor, P. Perona, D. Kriegman, and S. Belongie. Beyond pairwise clustering. In *CVPR*, 2005.
- [2] N. K. Ahmed, N. Duffield, T. L. Willke, and R. A. Rossi. On sampling from massive graph streams. *PVLDB*, 10(11):1430–1441, 2017.
- [3] N. K. Ahmed, J. Neville, R. A. Rossi, and N. Duffield. Efficient graphlet counting for large networks. In *ICDM*, 2015.
- [4] N. K. Ahmed, J. Neville, R. A. Rossi, N. G. Duffield, and T. L. Willke. Graphlet decomposition:

- Framework, algorithms, and applications. *Knowledge and Information Systems*, 50(3):689–722, 2017.
- [5] S. G. Aksoy, T. G. Kolda, and A. Pinar. Measuring and modeling bipartite graphs with community structure. *Journal of Complex Networks*, 5(4):581–603, 2017.
 - [6] I. Amburg, N. Veldt, and A. R. Benson. Hypergraph clustering with categorical edge labels. *TheWebConf*, 2020.
 - [7] C. Aslay, M. A. U. Nasir, G. De Francisci Morales, and A. Gionis. Mining frequent patterns in evolving graphs. In *CIKM*, 2018.
 - [8] A.-L. Barabási and R. Albert. Emergence of scaling in random networks. *science*, 286(5439):509–512, 1999.
 - [9] L. Becchetti, P. Boldi, C. Castillo, and A. Gionis. Efficient algorithms for large-scale local triangle counting. *TKDD*, 4(3):1–28, 2010.
 - [10] A. R. Benson, R. Abebe, M. T. Schaub, A. Jadbabaie, and J. Kleinberg. Simplicial closure and higher-order link prediction. *PNAS*, 115(48):E11221–E11230, 2018.
 - [11] A. R. Benson, D. F. Gleich, and J. Leskovec. Higher-order organization of complex networks. *Science*, 353(6295):163–166, 2016.
 - [12] A. R. Benson, R. Kumar, and A. Tomkins. Sequences of sets. In *KDD*, 2018.
 - [13] S. P. Borgatti and M. G. Everett. Network analysis of 2-mode data. *Social networks*, 19(3):243–270, 1997.
 - [14] M. Bressan, S. Leucci, and A. Panconesi. Motivo: fast motif counting via succinct color coding and adaptive sampling. *PVLDB*, 12(11):1651–1663, 2019.
 - [15] J. Bu, S. Tan, C. Chen, C. Wang, H. Wu, L. Zhang, and X. He. Music recommendation by unified hypergraph: combining social media information and music content. In *MM*, 2010.
 - [16] L. Chen, X. Qu, M. Cao, Y. Zhou, W. Li, B. Liang, W. Li, W. He, C. Feng, X. Jia, et al. Identification of breast cancer patients based on human signaling network motifs. *Scientific reports*, 3:3368, 2013.
 - [17] L. De Stefani, A. Epasto, M. Riondato, and E. Upfal. Trièst: Counting local and global triangles in fully-dynamic streams with fixed memory size. In *KDD*, 2016.
 - [18] M. Faloutsos, P. Faloutsos, and C. Faloutsos. On power-law relationships of the internet topology. *ACM SIGCOMM computer communication review*, 29(4):251–262, 1999.
 - [19] P. W. Holland and S. Leinhardt. A method for detecting structure in sociometric data. In *Social Networks*, pages 411–432. Elsevier, 1977.
 - [20] X. Hu, Y. Tao, and C.-W. Chung. Massive graph triangulation. In *SIGMOD*, 2013.
 - [21] X. Hu, Y. Tao, and C.-W. Chung. I/o-efficient algorithms on triangle listing and counting. *TODS*, 39(4):1–30, 2014.
 - [22] S. Huang, M. Elhoseiny, A. Elgammal, and D. Yang. Learning hypergraph-regularized attribute predictors. In *CVPR*, 2015.
 - [23] Y. Huang, Q. Liu, S. Zhang, and D. N. Metaxas. Image retrieval via probabilistic hypergraph ranking. In *CVPR*, 2010.
 - [24] T. Hwang, Z. Tian, R. Kuangy, and J.-P. Kocher. Learning on weighted hypergraphs to integrate protein interactions and gene expressions for cancer outcome prediction. In *ICDM*, 2008.
 - [25] S. Jain and C. Seshadhri. A fast and provable method for estimating clique counts using turán’s theorem. In *WWW*, 2017.
 - [26] M. Jha, C. Seshadhri, and A. Pinar. A space efficient streaming algorithm for triangle counting using the birthday paradox. In *KDD*, 2013.
 - [27] J. Jiang, Y. Wei, Y. Feng, J. Cao, and Y. Gao. Dynamic hypergraph neural networks. In *IJCAI*, 2019.
 - [28] U. Kang, C. E. Tsourakakis, A. P. Appel, C. Faloutsos, and J. Leskovec. Radius plots for mining tera-byte scale graphs: Algorithms, patterns, and observations. In *SDM*, 2010.
 - [29] G. Karypis, R. Aggarwal, V. Kumar, and S. Shekhar. Multilevel hypergraph partitioning: applications in vlsi domain. *TVLSI*, 7(1):69–79, 1999.
 - [30] G. Karypis and V. Kumar. Multilevel k-way hypergraph partitioning. *VLSI design*, 11(3):285–300, 2000.
 - [31] J. Kim, W.-S. Han, S. Lee, K. Park, and H. Yu. Opt: a new framework for overlapped and parallel triangulation in large-scale graphs. In *SIGMOD*, 2014.
 - [32] B. Klimt and Y. Yang. The enron corpus: A new dataset for email classification research. In *ECML PKDD*, 2004.
 - [33] S. Ko and W.-S. Han. Turbograph++ a scalable and fast graph analytics system. In *SIGMOD*, 2018.
 - [34] J. B. Lee, R. A. Rossi, X. Kong, S. Kim, E. Koh, and A. Rao. Graph convolutional networks with motif-based attention. In *CIKM*, 2019.
 - [35] J. Leskovec, J. Kleinberg, and C. Faloutsos. Graphs over time: densification laws, shrinking diameters and possible explanations. In *KDD*, 2005.
 - [36] D. Li, Z. Xu, S. Li, and X. Sun. Link prediction in social networks based on hypergraph. In *WWW*, 2013.
 - [37] L. Li and T. Li. News recommendation via hypergraph learning: encapsulation of user behavior and news content. In *WSDM*, 2013.
 - [38] P. Li and O. Milenkovic. Inhomogeneous hypergraph clustering with applications. In *NIPS*, 2017.
 - [39] P.-Z. Li, L. Huang, C.-D. Wang, and J.-H. Lai. Edmot: An edge enhancement approach for motif-aware community detection. In *KDD*, 2019.
 - [40] R. Mastrandrea, J. Fournet, and A. Barrat. Contact patterns in a high school: a comparison between data collected using wearable sensors, contact diaries and friendship surveys. *PloS one*, 10(9), 2015.
 - [41] R. Milo, S. Itzkovitz, N. Kashtan, R. Levitt, S. Shen-Orr, I. Ayzenshtat, M. Sheffer, and U. Alon. Superfamilies of evolved and designed networks. *Science*, 303(5663):1538–1542, 2004.
 - [42] R. Milo, S. Shen-Orr, S. Itzkovitz, N. Kashtan, D. Chklovskii, and U. Alon. Network motifs: simple building blocks of complex networks. *Science*, 298(5594):824–827, 2002.
 - [43] M. Ouyang, M. Toulouse, K. Thulasiraman, F. Glover, and J. S. Deogun. Multilevel cooperative search for the circuit/hypergraph partitioning problem. *TCAD*, 21(6):685–693, 2002.
 - [44] R. Pagh and C. E. Tsourakakis. Colorful triangle

- counting and a mapreduce implementation. *Information Processing Letters*, 112(7):277–281, 2012.
- [45] A. Paranjape, A. R. Benson, and J. Leskovec. Motifs in temporal networks. In *WSDM*, 2017.
- [46] A. Pinar, C. Seshadhri, and V. Vishal. Escape: Efficiently counting all 5-vertex subgraphs. In *WWW*, 2017.
- [47] R. A. Rossi, N. K. Ahmed, A. Carranza, D. Arbour, A. Rao, S. Kim, and E. Koh. Heterogeneous network motifs. *arXiv preprint arXiv:1901.10026*, 2019.
- [48] R. A. Rossi, N. K. Ahmed, and E. Koh. Higher-order network representation learning. In *TheWebConf Companion*, 2018.
- [49] S.-V. Sanei-Mehri, A. E. Sariyuce, and S. Tirthapura. Butterfly counting in bipartite networks. In *KDD*, 2018.
- [50] S. S. Shen-Orr, R. Milo, S. Mangan, and U. Alon. Network motifs in the transcriptional regulation network of escherichia coli. *Nature genetics*, 31(1):64–68, 2002.
- [51] K. Shin. Wrs: Waiting room sampling for accurate triangle counting in real graph streams. In *ICDM*, 2017.
- [52] K. Shin, S. Oh, J. Kim, B. Hooi, and C. Faloutsos. Fast, accurate and provable triangle counting in fully dynamic graph streams. *TKDD*, 14(2):1–39, 2020.
- [53] A. Sinha, Z. Shen, Y. Song, H. Ma, D. Eide, B.-J. Hsu, and K. Wang. An overview of microsoft academic service (mas) and applications. In *WWW*, 2015.
- [54] J. Stehlé, N. Voirin, A. Barrat, C. Cattuto, L. Isella, J.-F. Pinton, M. Quaggiotto, W. Van den Broeck, C. Régis, B. Lina, et al. High-resolution measurements of face-to-face contact patterns in a primary school. *PLoS one*, 6(8), 2011.
- [55] L. Sun, S. Ji, and J. Ye. Hypergraph spectral learning for multi-label classification. In *KDD*, 2008.
- [56] C. E. Tsourakakis, U. Kang, G. L. Miller, and C. Faloutsos. Doulion: counting triangles in massive graphs with a coin. In *KDD*, 2009.
- [57] C. E. Tsourakakis, J. Pachocki, and M. Mitzenmacher. Scalable motif-aware graph clustering. In *WWW*, 2017.
- [58] P. Wang, P. Jia, Y. Qi, Y. Sun, J. Tao, and X. Guan. Rept: A streaming algorithm of approximating global and local triangle counts in parallel. In *ICDE*, 2019.
- [59] P. Wang, Y. Qi, Y. Sun, X. Zhang, J. Tao, and X. Guan. Approximately counting triangles in large graph streams including edge duplicates with a fixed memory usage. *PVLDB*, 11(2):162–175, 2017.
- [60] D. J. Watts and S. H. Strogatz. Collective dynamics of small-world networks. *nature*, 393(6684):440, 1998.
- [61] H. Yang, B. Qu, J. Yang, and P. Cudre-Mauroux. Revisiting user mobility and social relationships in lbsns: A hypergraph embedding approach. In *TheWebConf*, 2019.
- [62] H. Yin, A. R. Benson, J. Leskovec, and D. F. Gleich. Local higher-order graph clustering. In *KDD*, 2017.
- [63] S.-e. Yoon, H. Song, K. Shin, and Y. Yi. How much and when do we need higher-order information in hypergraphs? a case study on hyperedge prediction. *TheWebConf*, 2020.
- [64] J. Yu, D. Tao, and M. Wang. Adaptive hypergraph learning and its application in image classification. *TIP*, 21(7):3262–3272, 2012.
- [65] Y. Yu, Z. Lu, J. Liu, G. Zhao, and J.-r. Wen. Rum: Network representation learning using motifs. In *ICDE*, 2019.
- [66] M. Zhang, Z. Cui, S. Jiang, and Y. Chen. Beyond link prediction: Predicting hyperlinks in adjacency space. In *AAAI*, 2018.
- [67] H. Zhao, X. Xu, Y. Song, D. L. Lee, Z. Chen, and H. Gao. Ranking users in social networks with higher-order structures. In *AAAI*, 2018.
- [68] D. Zhou, J. Huang, and B. Schölkopf. Learning with hypergraphs: Clustering, classification, and embedding. In *NIPS*, 2007.